HHS Public Access

Author manuscript

Nat Neurosci. Author manuscript; available in PMC 2012 November 01.

Published in final edited form as:

Nat Neurosci. 2012 May ; 15(5): 776–785. doi:10.1038/nn.3088.

Localized Microstimulation of Primate Pregenual Cingulate Cortex Induces Negative Decision-Making

Ken-ichi Amemori and **Ann M. Graybiel***

McGovern Institute for Brain Research, and Department of Brain and Cognitive Sciences, Massachusetts Institute of Technology, Cambridge, MA 02139

Abstract

The pregenual anterior cingulate cortex (pACC) has been implicated in human anxiety disorders and depression, but the circuit-level mechanisms underlying these disorders are unclear. We took as a clue evidence that in healthy individuals, the pACC is involved in cost-benefit evaluation. We developed a macaque version of an approach-avoidance decision task used to evaluate anxiety and depression in humans and, with multi-electrode recording and cortical microstimulation, we probed pACC function as monkeys performed this task. We found that the macaque pACC has an opponent-process like organization of neurons representing motivationally positive and negative subjective value. These two neuronal populations overlapped spatially, except in one pACC subzone, where neurons with negative coding were more numerous. Strikingly, microstimulation in this subzone, but not elsewhere in the pACC, increased negative decision-making, and this negative biasing was blocked by anti-anxiety drug treatment. This cortical zone could be critical for regulating negative emotional valence and anxiety in decision-making.

Many of the decisions that we make in daily life involve weighing benefits against the costs that they entail[1–3]. Even these everyday decisions can evoke anxiety[4], and in clinical conditions including anxiety disorders and depression, such decision-making is especially difficult[5]. For example, people suffering from anxiety make more plans based on expected negative consequences, and people suffering from depression make fewer plans based on expected rewards[6, 7]. Neuropsychological tasks requiring such cost-benefit evaluation, called approach-avoidance conflict tasks[2], have been designed to characterize these clinical and psychological states[8] and to quantify anxiolytic drug effects in animal models of anxiety[9]. Drugs that can increase approach decisions in approach-avoidance tasks are promising candidate anxiolytics, suggesting that the emotional state of anxiety is a crucial factor in approach-avoidance decision-making[5, 10, 11]. This suggests a functional link between potentiated anxiety states characteristic of neuropsychiatric conditions and the type of cost-benefit decision-making embodied in approach-avoidance tasks.

*To whom correspondence should be addressed. graybiel@mit.edu.

Contributions

K.A and A.M.G. designed the experiments and performed the surgeries; K.A. collected the data; and K.A and A.M.G analyzed the data and wrote the manuscript.

At the core of such approach-avoidance decision-making are judgments about the subjective value of the 'good' and 'bad' alternatives that are simultaneously confronted. An optimistic view leads to more approach decisions; a pessimistic view leads to more avoidance decisions. Decision variables are widely represented in the frontal cortex of macaque monkey[12, 13]. Especially for the dorsal part of the anterior cingulate cortex (ACC), many recording studies have shown that the ACC neurons can encode the gain[14] or cost[12] associated with expected outcomes[15, 16], as well as with prediction errors[17] and loss of reward[18]. In accord with these physiological studies, anatomical work suggests that the far-anterior, pregenual part of the anterior cingulate cortex (the pACC) has predominant connectivity with limbic as well as prefrontal regions[19–21]. We recorded in these regions, but focused on the ventral bank of the anterior cingulate sulcus because this region has been implicated in humans in cost-benefit decisions[22–24] as well as in emotional responses triggered by conflict situations[25, 26], and has anatomical connections with striosomes of the caudate nucleus[20].

The fact that the pACC is involved in both cost-benefit decision-making and emotional regulation suggests a potential function for the pACC in controlling emotional state. Consistent with this view, evidence of a correlation between abnormal pACC activity and anxiety-related disorders has emerged in human neuropsychiatric studies[27]. The pACC has been implicated in anxiety-related disorders including obsessive-compulsive disorder[28], post-traumatic stress disorder[29], addiction[30] and major depression[27]. In particular, activity in the pACC has been found to predict clinical response to antidepressant treatments[31, 32], and it is thought to be affected indirectly by deep brain stimulation of the subgenual ACC applied as a therapy for depression[33]. Yet the neuronal mechanisms operating in the pACC to affect emotional anxiety and emotional decision-making remain largely unknown.

In the experiments that we describe here, we developed a cost-benefit decision-making task for macaque monkeys modeled after the approach-avoidance protocols used in human cognitive science to quantify the degree of anxiety about the outcome of decision-making. With combinations of multi-electrode recording, cortical microstimulation and anxiolytic drug treatment, we sought to identify characteristics of the pACC that could underlie a functional interplay between anxiety-related emotional processes and decision-making.

RESULTS

Decision-making in the approach-avoidance task

We first recorded behavior and neural spike activity in the pACC in two macaque monkeys (S and A) as they performed a novel approach-avoidance (Ap-Av) task in which they made decisions to approach or to avoid combinations of positive (food) and negative (airpuff) outcomes cued in advance by visual stimuli during a decision period (Fig. 1a; **Methods**). The monkeys looked at a cue composed of contiguous red and yellow bars whose lengths linearly corresponded to the amount of food (red bar) and the strength of the airpuff (yellow bar) that would be delivered at the end of the trial. They could then choose to approach or to avoid the combinations by moving a cursor. After approach decisions, both food and airpuff were delivered in the indicated amounts. After avoidance decisions, the monkeys did not

receive the indicated food and airpuff, but only a standard minimum food amount, necessary to maintain motivation to perform the task.

The monkeys systematically varied their decisions to approach or to avoid depending on the relative sizes of the food rewards and airpuffs indicated by the cues. Fig. 2a shows a scatter plot of decisions made by monkey S during a block of trials in the Ap-Av task, and Fig. 2b illustrates the decisions made in the Ap-Av block averaged across sessions. Based on Bayesian information criteria (Supplementary Fig. 1), we adopted the logistic behavioral model that could best characterize the behavioral choice of monkey. With this model, the decision boundary between approach and avoidance decisions was linear (black line in Fig. 2a; dotted line in Fig. 2b). The fact that the mean reaction times increased along the decision boundary indicated conflict in the monkey's decision-making, especially for low values of indicated reward (Fig. 2c).

To test whether these approach-avoidance decisions could be influenced by drugs that relieve anxiety in humans[5], we administered the anxiolytic drug, diazepam[10], to two monkeys (monkeys S and P) during 14 sessions (Supplementary Fig. 2). Diazepam treatment increased the monkey’s approach decisions in the Ap-Av task by an average of 7 %, measured by the size of significant change in decision in the decision matrix (i.e., the matrix of decision relative to offered reward and airpuff, see **Methods**), and these effects were dose-dependent. Saline treatment was without effect, yielding significant differences between the diazepam and saline treatments (t-test, $P < 0.001$). These results suggest that the behavioral response induced in the monkeys by approach-avoidance decision-making could be regulated by an anxiolytic drug[9], a result raising the interpretative possibility that the task in monkeys, as in humans, tapped into some anxiety-like state.

As a control decision-making task, we designed an approach-approach (Ap-Ap) task that was identical to the Ap-Av task except that the red and the yellow bars both signaled potential reward amounts (Fig. 1b). The rewards offered by the red bar and the yellow bar were obtained, respectively, by choosing cross and square targets. So as to have the decision boundaries similar to those in the Ap-Av task, the reward amount offered per unit length of the red bar was adjusted to be double the reward amount offered by the equivalent length of the yellow bar (Fig. 2d,e). Reaction times increased around the decision boundaries, also especially when the monkeys were offered smaller amount of reward than that they obtained on average (Fig. 2f). In sharp contrast to decision-making in the Ap-Av task, the Ap-Ap decisions were not affected by treatment with diazepam at any dose used (Supplemental Fig. 2). Thus the observed behaviors of the monkeys were comparable in the Ap-Av and Ap-Ap tasks, but the pharmacologic treatments suggested that the monkeys could have been subject to different types of subjective state while performing the two different decision-making tasks.

Neural activity during the decision-making tasks

We recorded the activity of 1065 well-isolated single units in the pACC and adjoining medial prefrontal cortex of monkeys S and A (Fig. 1d) with chronically implanted electrodes as they performed alternating 150-trial blocks of the Ap-Av and Ap-Ap tasks (Supplementary Fig. 3). We focused on analyzing the activities of task-related units having

mean firing rates during the cue period that were significantly different from those recorded in the baseline 1-s intertrial period before trial initiation or in the 1.5-s pre-cue fixation period (two-tailed t-test, $P < 0.05$). Over three-quarters of recorded units (82.2%, 875/1065) were task-related according to this criterion. Because initial analyses showed that neuronal activities were affected by task condition (Supplementary Fig. 4), we focused on the Ap-Av task.

We used stepwise regression analyses to determine whether unit firing rates during the cue period of the Ap-Av task were correlated with observable task variables: 'offered reward' (the amount of offered reward indicated by the red bar, Rew) and 'offered airpuff' (the strength of offered airpuff indicated by the yellow bar, Ave), the binary value of approach (Cho=1) or avoidance (Cho=0), 'chosen reward' (the amount of chosen reward, Cho*Rew), 'chosen airpuff' (the strength of chosen airpuff, Cho*Ave), and the reaction times (RT). In addition, we introduced two hypothetical subjective variables: expected utility (Eutil) and conflict in decision (Conf), considering the characteristics of the Ap-Av task. First, we reasoned that in the Ap-Av task, if the pACC were to mediate cost-benefit integration, then it was likely that pACC neurons would represent both offered and chosen values[34, 35]. To derive the subjective value of the chosen target, or utility, we approximated the behavior by the conditional logit model[36] and inferred utility inversely[37] (Supplementary Note). We then used expected utility[38] as an explanatory variable that corresponds to the continuous form of 'chosen value'[35]. We also performed a pilot test using stepwise regression with variables including utility of each option, and found that none of these units had activity characterized by option utility. Second, we considered whether the pACC were involved in monitoring conflict[39], especially when decisions had to be made between two options with similar offered values[2]. To search for pACC units encoding such 'conflict in decision', we introduced the calculated information entropy of decision-making as an indicator of decision conflict, and used this as an explanatory variable.

Stepwise regression analyses (Supplementary Note) indicated that among 875 task-related units, many (556 units, 63.5%) had activity during the decision period of the Ap-Av task that was significantly well characterized by linear combinations of these eight factors (F-test, $P < 0.05$; Fig. 3a). Among these, the majority (397 units, 71.4%) had activity patterns that were characterized by one of these variables. Because many of these units were uniquely characterized by a single variable, but not by a combination of these variables, the majority of units encoded, within the detection limits of the regression model, a single factor specifically characterized by the variable. We focused on the 397 units that had cue-period activity accounted for by single variables (Supplementary Fig. 5).

Classification of pACC unit activity

We next asked whether there was a property of their response patterns during the decision period that was shared across the different types of units. We applied multidimensional scaling (MDS) to quantify the similarity of their firing patterns and categorized them based on their similarity (Fig. 3b). Two principal features derived by the MDS accounted for nearly all of the variability across different types of units, and most of the features were accounted for by the first principal dimension (Supplementary Fig. 6). Moreover, in the

first-feature dimension (x-axis of Fig. 3b), nearly all unit types fell into two clear clusters: the units that were positively correlated with the regression variables, and the units negatively correlated with the regression variables. We thus categorized the pACC unit populations as P-type (units positively correlated with the principal feature in the orange region of Fig. 3b) and N-type (units negatively correlated with the principal feature in the blue region of Fig. 3b). Examples are shown in Supplementary Fig. 7. The two outliers in this first principle feature analysis were accounted for by the second principal feature: units with activity positively or negatively correlated to the offered airpuff (Ave) were almost maximally distant on the dimension defined by the second principal feature (y-axis of Fig. 3b).

P-type units exhibited spike activity that was correlated with variables that preceded or followed approach decisions. They were activated when the monkeys were offered large reward (high Rew), expected high value for the outcome (high Eutil), were about to decide to approach (Cho=1), or were ready to receive reward (high Cho*Rew) and airpuff (high Cho*Ave). These variables thus appeared to be consistently related to the causes or effects of positive motivational states. We thus refer to the variable that activates P-type units as a "motivationally positive" variable. Conversely, N-type units consisted of units with activities correlated with variables that led or followed avoidance decisions. They were activated when the monkeys were offered small reward (low Rew), expected low value for the outcome (low Eutil), or were about to decide to avoid (Cho=0). They were also activated when the decision was variable, indicating potentially subjective conflict (high Conf) and when the reaction times were prolonged (high RT). These behavioral variables thus appeared to be related to negative motivational states. We thus refer to the variables that activate N-type units as "motivationally negative" variables.

These results suggested that many units in the pACC could be divided into distinct populations of neurons related to cost-benefit decision-making. When we mapped the spatial distributions of these N-type and P-type populations within the pACC region sampled, we found that the P-type and N-type units had largely similar spatial distributions within the pACC (Fig. 3c). However, there was one clear exception: in the region of the ventral bank of the cingulate sulcus (blue region in Fig. 3c), the N-type units were differentially enriched relative to the P-type units (Fisher's exact test, $P < 0.05$).

Firing patterns of N-type and P-type units

To characterize the representative properties of these two distinct populations of pACC neurons, we examined their activity profiles during the cue period (Fig. 4). In the Ap-Av task, the N-type population responded to visual cues that subsequently were followed by an avoidance decision, and they responded maximally to visual cues offering low food and low airpuff (Fig. 4a). The responses of N-type unit population were task-dependent: in the Ap-Ap task, they responded only to visual cues offering low food rewards (Fig. 4b). Under these conditions, both the frequency of omission errors (Supplementary Fig. 8) and the monkeys' reaction times (Fig. 2c,f) increased, suggesting that they might have been relatively less motivated, experiencing conflict or possible frustration with the low yields cued. The P-type population, by contrast, responded to cues that were followed by approach in the Ap-Av task

and fired maximally to the cues that offered large reward and weak airpuff (Fig. 4f). Like the N-type population, the P-type population changed their activity depending on the task version. In the Ap-Ap task, they responded to long red and yellow bars offering large amounts of reward (Fig. 4g).

This pattern of results suggested that expected utility might provide a more comprehensive construct to account for the firing patterns[34, 35]. We therefore performed correlation analyses between expected utility and the activity of N-type and P-type units in the Ap-Av and Ap-Ap tasks. For each N-type unit (Fig. 4c,d), we calculated the correlation coefficient between the cue-period firing rate in the Ap-Av task and the expected utility calculated for the Ap-Av task (x-axis of Fig. 4e). The mean of the distribution of the correlation coefficients (r(Eutil, Ap-Av)) was significantly negative (two-tailed t-test, $P < 10^{-56}$). For the same individual units, we calculated the correlation coefficients between the cue-period activity in the Ap-Ap task and the expected utility for the Ap-Ap task (y-axis of Fig. 4e), Notably, the mean of the correlation distribution (r(Eutil, Ap-Ap)) was also significantly negative (two-tailed t-test, $P < 10^{-17}$). The N-type population included 45 single units with activities significantly correlated with the expected utility in both task versions (Pearson's correlation coefficients, $P < 0.05$). Moreover, the correlation distributions for the Ap-Av task and the Ap-Ap task were themselves significantly correlated ($r = 0.49$, $P < 10^{-12}$; Fig. 4e).

Similarly, as shown in Fig. 4j, for each P-type unit (Fig. 4h,i), we calculated the correlation distributions between cue-period activity and expected utility in both tasks: r(Eutil, Ap-Av) and r(Eutil, Ap-Ap). The mean of the correlation distribution in the Ap-Av task (r(Eutil, Ap-Av)) was significantly positive (two-tailed t-test, $P < 10^{-42}$), and the mean of the correlation distribution in the Ap-Ap task (r(Eutil, Ap-Av)) was as well (two-tailed t-test, $P < 10^{-22}$). There were 53 units in the P-type population that had activities significantly correlated with the expected utility in both task versions ($P < 0.05$). The correlation distributions for the population activity in the two populations were again significantly correlated with each other ($r = 0.56$, $P < 10^{-13}$). Together, these findings suggested that the populations of N-type and P-type pACC units were activated in relation to the subjective value of chosen outcome, but with contrasting negative and positive coding schemes that were robustly expressed across the two tasks.

Distribution of negative and positive unit-coding

If the pACC did contain a decision mechanism based on complementary positive and negative representations of expected utility, then the border between the subjective cost and benefit of the decisions could be set by the balance of activity of the N-type and P-type units[40]. In most pACC regions sampled, N-type and P-type units were apparently evenly intermixed, but N-type units predominated over P-type units in the ventral bank of the cingulate sulcus (Fig. 3c).

To determine whether this biased distribution toward negatively correlated units in the ventral bank region was produced by units with one primary behavioral correlate, or instead, by units with activity correlated with multiple behavioral variables, we performed a series of correlation analyses between unit activity and each behavioral variable used in the

regression analyses. For each variable, we tested whether there was a predominance of ventral bank units with activity either positively or negatively correlated with the given variable. Fig. 5 shows the distributions of units with significant correlations (Pearson's correlation coefficients, $P < 0.05$). The results were striking. Negatively correlated units predominated positive ones in the ventral bank (Fisher's exact test, $P < 0.05$) for offered reward (Rew, Fig. 5a), for expected utility (Eutil, Fig. 5c), and for chosen reward amount (Cho*Rew, Fig. 5e). For conflict in decision (Conf, Fig. 5g) and for reaction time (RT, Fig. 5h), positively correlated units dominated negative ones. And for decision (Cho, Fig. 5d), units coding avoidance (Cho=0) dominated units coding approach (Cho=1). Thus, except for offered and chosen airpuff strength (Ave, Fig. 5b and Cho*Ave, Fig. 5f), units responding to multiple different variables (low Rew, low Eutil, low Cho*Rew; high Conf and high RT; Cho=0) predominated over their counterparts in the ventral bank region. These variables corresponded to the "motivationally negative" variables that activated N-type units.

Microstimulation alters approach-avoidance decision-making

Based on these biased distributions, we reasoned that microstimulation in this ventral bank zone might bias the monkeys' decision-making toward avoidance decisions, whereas stimulation elsewhere in the sampled pACC region might have limited effect due to the balance between the N-type and P-type populations. To test this prediction, we microstimulated at 97 sites in the pACC of monkeys S and A, using 1-s-long trains of biphasic pulses that started at the onset of the visual cues (Fig. 1c). Each site was stimulated in successive daily Ap-Av ($n = 97$) and Ap-Ap ($n = 31$) sessions. Within individual sessions, we alternated stimulation-off and stimulation-on trials in blocks of 250 trials.

The effects of the microstimulation on the monkeys' decision-making were remarkably selective. Stimulation was effective almost exclusively during performance of the Ap-Av task, it produced almost exclusively an increase in avoidance decisions, and it produced this effect almost exclusively for stimulation applied to the ventral bank of the cingulate sulcus (Figs. 6 and 7). Fig. 6 shows the results from a single stimulation site in the ventral bank region. Compared to the stimulation-off trials (Fig. 6a), the slope of the decision boundary during the stimulation-on trials was shifted rightward, and the number of avoidance decisions was increased (Fig. 6b). To quantify the effect of the stimulation, we introduced a spatial smoothing method and used Fisher's exact probability test (**Methods**). We defined effective sites as those for which stimulation changed the monkey's decisions significantly ($P < 0.05$) for at least 5% of all combinations of the two cues. Microstimulation in the ventral bank of the cingulate sulcus significantly increased avoidance choices for 16.6% of all cue combinations, most strongly for those indicating high airpuff strengths (Fig. 6c). Identically applied stimulation at the same site during Ap-Ap task performance did not induce any change in decision (Fig. 6d–f).

Of the 97 sites examined in the medial wall cortex, 15 sites were effective, 13 of these (86.7%) produced an increase in avoidance, and all 13 were in the ventral bank of the cingulate sulcus (Fig. 7a; Supplementary Fig. 9). To characterize the stimulation effects at these 13 effective sites, all the behavioral data were accumulated (Supplementary Fig. 10) and, with the accumulated data, the difference in decision-making between stimulation-on

and stimulation-off trials was expressed as t-scores. The tendency for increased avoidance in the Ap-Av task was positively correlated with the strength of the aversive airpuff indicated by the visual cues (Fig. 7b), but was unchanged in the Ap-Ap task (Fig. 7c). Reaction times were affected in both monkeys, most strongly in monkey S, and were, in both, larger for high-conflict decisions than for low-conflict decisions (Supplementary Fig. 11). In some experiments, we ran triple-session experiments with successive days of Ap-Av, Ap-Ap and Ap-Av tasks, and confirmed that differential results of two tasks were consistently observed (Supplementary Fig. 12a). For two sites at which we found increased approach on stimulation, the effects were about 5% (blue circles, Fig. 7a).

Cumulative effects of microstimulation on decision-making

What could account for this highly selective biasing in decisions toward avoidance? Classical electrical stimulation studies showed that electrical stimulation of the rostral ACC evokes changes in autonomic signs, including skin conductance[41]. However, we found no changes in skin conductance induced by the microstimulation (Supplementary Fig. 12b,c), suggesting that the microstimulation we used was too weak to induce strong fear or pain. We did note an increased incidence of 'coo' vocalization[41] in some sessions, consistent with this pACC region's known importance for vocalization and social communication[42].

A clue to the origin of the increased avoidance behavior came from another set of experiments in which we randomly alternated the stimulation-on and stimulation-off trials within a given session. We found little difference between the stimulation-on and stimulation-off decisions (Fig. 7d). However, when we compared the averaged decision boundaries for random stimulation experiments to the decision boundaries calculated in the prior normal sessions from pooled stimulation-off trials (e.g., Fig. 7b), we found that the boundaries for the random experiments were biased toward avoidance. This unexpected result suggested that the effect of the randomized stimulation persisted to affect the following stimulation-off trials. We therefore tested, in the standard block-design, whether the stimulation effects were cumulative. They were (Fig. 7e). These accumulating effects raised the possibility that pACC stimulation could bring about a tonic, persistent state affecting the relative evaluation of cost and benefit.

Blockade of induced negative decisions by anxiolytic

These results in turn raised the possibility that such a persistent state could be influenced by anxiolytic treatment. We tested this possibility in another set of experiments by asking whether anxiolytics could reduce the stimulation effects (Fig. 8a). We divided Ap-Av sessions into three successive 200-trial blocks: stimulation-off, stimulation-on and stimulation-on after drug administration. Between the second and third blocks, we administered the anxiolytic, diazepam (0.25 mg/kg, IM). We represented the effect of microstimulation by the change in the decision matrix between the first and second blocks (Fisher's exact test, $P < 0.05$), and the effect of stimulation plus drug by the change in decision between the first and third blocks. In two experiments, we stimulated an effective ventral bank site with 80 μA current (site A; orange lines with square terminals in Fig. 8a; location marked in Fig. 8b). We consistently observed an increase in avoidance decisions, especially for high-conflict regions, and in each session, this stimulation effect was fully

blocked by the diazepam administration. In a third experiment (Supplementary Fig. 13), we stimulated the same site with a higher current amplitude (150 μA), and obtained a larger effect of the microstimulation. This effect was not only blocked by the anxiolytic, but reversed: now the microstimulation produced increased approach decisions (Fig. 8a, orange line with circle terminals). Finally, in a fourth experiment, we stimulated at a site previously identified as non-effective (80 μA; site B; location marked in Fig. 8b). We found no change in the monkey's decisions (black line in Fig. 8a), but confirmed an increase in approach by diazepam administration.

We next applied the logistic behavioral model chosen for the main experiments (**Methods**) to the data obtained in the stimulation-off and stimulation-on sessions to compare the change in sensitivities to cost (airpuff) and benefit (reward). In the model, the cost-benefit ratios were taken as the slopes of the decision boundaries of the logistic model. The anatomical sites of stimulation at which the model showed an increase in cost-benefit ratio (decreased slope of the decision boundary) matched closely the sites at which increased avoidance was actually found experimentally (Fig. 8b). The model suggested that the microstimulation enhanced sensitivity to offered airpuff relative to offered reward primarily around the ventral bank effective zone in which we had found more N-type units in our recording experiments. These findings suggest that the microstimulation of the ventral bank pACC neurons could have led to a negative biasing of cost-benefit evaluation.

Discussion

Our findings suggest that neurons in the macaque pACC can be divided into populations representing two poles of an opponent-process evaluation mechanism. Depending on whether their cue-period responses were greater for cost-related variables or for benefit-related variables in the Ap-Av task, the pACC neurons could be separated into two broad groups, the N-type and P-type neuronal populations. Those neurons encoding motivationally negative (N) and positive (P) variables were widely distributed within the pACC, and were apparently intermixed with one another, as would be appropriate for components of a decision-making neuronal mechanism[40]. However, there was one exception to this symmetric distribution of the N-type and P-type units: in the pregenual zone within the ventral bank of the cingulate sulcus, there were significantly more neurons that, across nearly the full range of variables examined, represented negative motivational variables more than positive ones. It was in this ventral bank zone alone, of all pACC sites explored, that electrical microstimulation altered the approach-avoidance decisions made by the monkeys, specifically biasing them toward avoidance of the anticipated outcome. This effect of the microstimulation accumulated over time, suggesting that the effect represented a persistent state variable. Anxiolytic drug treatment blocked the effects of such microstimulation, suggesting that the stimulation could have induced an anxiety-like state. Collectively, these findings suggest that this localized ventral bank region of the pACC is differentially involved in weighing cost against benefit in situations requiring approach-avoidance decision-making, and suggest that excessive activation of this region can induce pessimistic evaluation of offered outcomes.

The stimulation effect selectively observed in the Ap-Av task should reflect its special characteristics. In the Ap-Av task, approach and avoidance options were directly associated with the monkey's subjective estimation of cost and benefit. The microstimulation changed the decisions by reducing the slope of the decision boundary, suggesting that the stimulation increased the subjective weighting of cost relative to benefit in the computations leading to outcome evaluation. Thus, the change in slope might have reflected an effect of the stimulation in devaluing benefit of reward relative to cost, for example, by reducing the general level of animal's motivation to seek reward. Alternatively, the stimulation might have induced subjective over-estimation of cost relative to benefit. We favor this second alternative, because treatment with the anxiolytic, diazepam, blocked and even reversed the increase in avoidance decision-making induced by microstimulation, and because such an effect is regarded to be primarily due to inhibition of anxiety[11]. If the monkeys felt increased anxiety about the consequences of their decision-making as a result of the microstimulation, it is reasonable that the stimulation could have augmented the negative value of chosen outcome—a negative biasing in expected utility. According to this working hypothesis, we suggest that the microstimulation could have led the monkeys to make pessimistic predictions about the consequence of their decisions by inducing an anxiety-like state.

In contrast to the Ap-Av task, the Ap-Ap task had no option associated with cost. Consistent with this task structure, the microstimulation that had increased the cost-benefit ratio in the Ap-Av task did not affect decision-making in the Ap-Ap task. However, despite the absence of behavioral change, the N-type and P-type populations were activated in the Ap-Ap task. These activities suggest that, irrespective of the task type, these units generally evaluate whether the consequence of an upcoming decision is ‘good’ or ‘bad’ relative to one's expectation. This view suggests that the cost-benefit boundary could have been set by balanced activity of N-type and P-type populations, flexibly changing depending on the average offers in each task.

The proposal that the pACC is involved in cost-benefit evaluation rather than specifically in option selection is also supported by the types of units that we observed in the pACC. With stepwise regression, we characterized pACC units representing 'offered cost' (Ave), 'offered benefit' (Rew) and 'chosen value' (Eutil), suggesting that the pACC contains units involved in cost-benefit integration to derive motivational value. Interestingly, those units were intermingled with units representing consequential motivational responses such as 'anticipation of each outcome' (Cho*Rew and Cho*Ave), 'emotional conflict' (Conf) and 'modulation of reaction time' (RT). Because units that uniquely encode targeted selection were not dominant, the function of the pACC might be characterized by cost-benefit integration necessary to derive a subjective value that could control multiple motivational processes.

We note that, to derive utility, we employed the conditional logit model and approximated the choice behavior. Though the model could account for the behavior with significant accuracy (Supplementary Note), the utility was not directly derived from the behavior. Further, because we did not vary the reward amount for avoidance option, we could not express utility in terms of primary reward values. Thus, the utility that we derived was specific to the task-context of our experiments.

A remarkable finding that emerged from our recording and stimulation maps is that within the broad pACC zone explored, neurons encoding negative motivational variables were differentially concentrated in the ventral bank of the cingulate sulcus, the region in which we found microstimulation to induce an increase in avoidance decisions. This biased distribution suggests one possible answer to questions of why the stimulation only induced avoidance and why the stimulation was effective selectively in the ventral bank. According to this view, stimulation of the ventral bank pACC zone over-activated pACC neurons representing negative motivational values, leading to a pessimistic evaluation of future outcome and to increase avoidance. Among the 97 pACC sites stimulated, we found increases in approach decisions only at two. These rare instances suggest that there could be pACC or other nearby zones in which stimulation would push the balance of decision-making toward approach decisions.

However, the neuronal mechanisms underlying the stimulation-induced changes are still unclear. The effects could depend not only on circuits within the pACC, but also on the brain regions downstream of the effective pACC stimulation zone. The effective zone lies within the rostral part of area 24 and the dorsal part of area 32. These are interconnected with other cortical regions implicated in decision-making, emotion and motivation[19, 43], including the dorsal part of the dorsolateral prefrontal cortex, implicated in cognitive and motivational planning[44], and the orbitofrontal cortex, implicated in stimulus evaluation[34]. The pACC region is also interconnected with the subgenual region of the anterior cingulate cortex, which has been targeted by electrical deep brain stimulation therapy for treatment-resistant depression[33]. These connections, however, are not selective for the zone in which we found microstimulation to bias the monkeys' decisions.

Strikingly, the effective ventral bank zone does appear unique in that it corresponds to the one subregion of the pACC previously identified as projecting preferentially to striosomes in the caudate nucleus[20]. This striosome link could provide preferential access to the dopamine-containing neurons of the substantia nigra directly[45] and indirectly via the lateral habenula[46, 47], itself a brain site related to negative reward prediction error[48]. The ventral bank of the cingulate sulcus also shares connectivity patterns with the amygdala[21], a brain region recognized as representing emotional valence[49, 50]. The predominance of avoidance in response to the over-activation of the ventral bank pACC cortex suggests that this zone could provide cortical control over such downstream circuitry. Signaling cascades for negative emotional decision-making could thus possibly originate in this localized pACC region. If so, it could represent the head-end of the rostral striosomal system.

The pACC in the human has been implicated, along with the subgenual ACC[33], in major depression[31, 32] and in anxiety-related disorders including obsessive-compulsive disorder[28] and post-traumatic stress disorder[29] as well as in addictive states[30]. Notably, increased activity in the pACC has been associated with beneficial response to a variety of antidepressant pharmacologic treatments[31]. Given our findings, the responsive pACC subregion identified here in the non-human primate could be a good candidate site for interrelating cognitive and emotional processing to modulate behavior by affecting evaluation of aversive outcome.

Supplementary Material

Refer to Web version on PubMed Central for supplementary material.

Acknowledgements

We thank Dr. Satoko Amemori and Margo Cantor for their help with animal training and surgical procedures, Drs. Patrick Tierney, Hideki Shimazu, Theresa Desrochers, Joseph Feingold and Yoshihisa Ninokura, and Henry Hall for their technical advice, and Drs. Diego Pizzagalli, Robert Desimone, Ki Goosens, Jesse Goldberg, Donald Pfaff, and Yasuo Kubota for reading the manuscript in draft form. This work was supported by NIH Javits Merit Grant (R01 NS025529), the Office of Naval Research (N000140710903), the Lynn Diamond Fellowship of the National Parkinson Foundation, and Mr. Ira J. Jaffe.

References

1. Lewin, KZ. A dynamic theory of personality. New York: McGraw-Hill; 1935.
2. Miller, NE. Selected papers on conflict, displacement, learned drives and theory. Chicago, Illinois: Aldine Atherton; 1971.
3. Elliot, AJ. Handbook of approach and avoidance motivation. New York: Psychology Press; 2008.
4. Elliot AJ, Thrash TM. Approach-avoidance motivation in personality: approach and avoidance temperaments and goals. J Pers Soc Psychol. 2002; 82:804–818. [PubMed: 12003479]
5. Millan MJ. The neurobiology and control of anxious states. Prog in Neurobiol. 2003; 70:83–244.
6. Dickson JM. Perceived consequences underlying approach goals and avoidance goals in relation to anxiety. Pers Indiv Differ. 2006; 41:1527–1538.
7. Dickson JM, MacLeod AK. Approach and avoidance goals and plans: their relationship to anxiety and depression. Cognitive Ther Res. 2004; 28:415–432.
8. Ottenbreit ND, Dobson KS. Avoidance and depression: the construction of the cognitive-behavioral avoidance scale. Behav. Res. Ther. 2004; 42:293–313. [PubMed: 14975771]
9. Vogel JR, Beer B, Clody DE. A simple and reliable conflict procedure for testing anti-anxiety agents. Psychopharmacology. 1971; 21:1–7.
10. Rowlett JK, Lelas S, Tornatzky W, Licata SC. Anti-conflict effects of benzodiazepines in rhesus monkeys: relationship with therapeutic doses in humans and role of GABAA receptors. Psychopharmacology. 2006; 184:201–211. [PubMed: 16378217]
11. Treit D. Animal models for the study of anti-anxiety agents: a review. Neurosci. Biobehav. Rev. 1985; 9:203–222. [PubMed: 2861589]
12. Kennerley SW, Dahmubed AF, Lara AH, Wallis JD. Neurons in the frontal lobe encode the value of multiple decision variables. J Cogn Neurosci. 2008; 21:1162–1178. [PubMed: 18752411]
13. Kennerley SW, Wallis JD. Evaluating choices by single neurons in the frontal lobe: outcome value encoded across multiple decision variables. Eur J Neurosci. 2009; 29:2061–2073. [PubMed: 19453638]
14. Hayden BY, Platt ML. Neurons in anterior cingulate cortex multiplex information about reward and action. J. Neurosci. 2010; 30:3339–3346. [PubMed: 20203193]
15. Seo H, Lee D. Temporal filtering of reward signals in the dorsal anterior cingulate cortex during a mixed-strategy game. J. Neurosci. 2007; 27:8366–8377. [PubMed: 17670983]
16. Ito S, Stuphorn V, Brown JW, Schall JD. Performance monitoring by the anterior cingulate cortex during saccade countermanding. Science. 2003; 302:120–122. [PubMed: 14526085]
17. Matsumoto M, Matsumoto K, Abe H, Tanaka K. Medial prefrontal cell activity signaling prediction errors of action values. Nat Neurosci. 2007; 10:647–656. [PubMed: 17450137]
18. Hayden BY, Pearson JM, Platt ML. Fictive reward signals in the anterior cingulate cortex. Science. 2009; 324:948–950. [PubMed: 19443783]
19. Vogt BA, Pandya DN. Cingulate cortex of the rhesus monkey: II. Cortical afferents. J Comp Neurol. 1987; 262:271–289. [PubMed: 3624555]

20. Eblen F, Graybiel AM. Highly restricted origin of prefrontal cortical inputs to striosomes in the macaque monkey. J Neurosci. 1995; 15:5999–6013. [PubMed: 7666184]
21. Ghashghaei HT, Hilgetag CC, Barbas H. Sequence of information processing for emotions based on the anatomic dialogue between prefrontal cortex and amygdala. Neuroimage. 2007; 34:905–923. [PubMed: 17126037]
22. Tom SM, Fox CR, Trepel C, Poldrack RA. The neural basis of loss aversion in decision-making under risk. Science. 2007; 315:515–518. [PubMed: 17255512]
23. Croxson PL, Walton ME, O'Reilly JX, Behrens TE, Rushworth MF. Effort-based cost-benefit valuation and the human brain. J. Neurosci. 2009; 29:4531–4541. [PubMed: 19357278]
24. Talmi D, Dayan P, Kiebel SJ, Frith CD, Dolan RJ. How humans integrate the prospects of pain and reward during choice. J. Neurosci. 2009; 29:14617–14626. [PubMed: 19923294]
25. Bush G, Luu P, Posner MI. Cognitive and emotional influences in anterior cingulate cortex. Trends Cogn Sci. 2000; 4:215–222. [PubMed: 10827444]
26. Etkin A, Egner T, Peraza DM, Kandel ER, Hirsch J. Resolving emotional conflict: a role for the rostral anterior cingulate cortex in modulating activity in the amygdala. Neuron. 2006; 51:871–882. [PubMed: 16982430]
27. Pizzagalli DA. Frontocingulate dysfunction in depression: toward biomarkers of treatment response. Neuropsychopharmacology. 2011; 36:183–206. [PubMed: 20861828]
28. Fitzgerald KD, et al. Error-related hyperactivity of the anterior cingulate cortex in obsessive-compulsive disorder. Biol Psychiat. 2005; 57:287–294. [PubMed: 15691530]
29. Kasai K, et al. Evidence for acquired pregenual anterior cingulate gray matter loss from a twin study of combat-related posttraumatic stress disorder. Biol Psychiatry. 2008; 63:550–556. [PubMed: 17825801]
30. Goldstein RZ, et al. Anterior cingulate cortex hypoactivations to an emotionally salient task in cocaine addiction. Proc Natl Acad Sci USA. 2009; 106:9453–9458. [PubMed: 19478067]
31. Mayberg HS, et al. Cingulate function in depression: a potential predictor of treatment response. NeuroReport. 1997; 8:1057–1061. [PubMed: 9141092]
32. Pizzagalli D, et al. Anterior cingulate activity as a predictor of degree of treatment response in major depression: evidence from brain electrical tomography analysis. Am J Psychiat. 2001; 158:405–415. [PubMed: 11229981]
33. Mayberg HS, et al. Deep brain stimulation for treatment-resistant depression. Neuron. 2005; 45:651–660. [PubMed: 15748841]
34. Padoa-Schioppa C, Assad JA. Neurons in the orbitofrontal cortex encode economic value. Nature. 2006; 441:223–226. [PubMed: 16633341]
35. Padoa-Schioppa C. Neurobiology of economic choice: a good-based model. Annu. Rev. Neurosci. 2011; 34:333–359. [PubMed: 21456961]
36. McFadden, D. Conditional logit analysis of qualitative choice behavior. In: Zarembka, P., editor. Frontiers in econometrics. New York: Academic Press; 1974. p. 105-142.
37. Levy I, Snell J, Nelson AJ, Rustichini A, Glimcher PW. Neural representation of subjective value under risk and ambiguity. J. Neurophysiol. 2010; 103:1036–1047. [PubMed: 20032238]
38. Von Neumann, J.; Morgenstern, O. Theory of games and economic behavior. Princeton: Princeton Univ. Press; 1947.
39. Botvinick MM, Cohen JD, Carter CS. Conflict monitoring and anterior cingulate cortex: an update. Trends Cogn. Sci. 2004; 8:539–546. [PubMed: 15556023]
40. Machens CK, Romo R, Brody CD. Flexible control of mutual inhibition: a neural model of two-interval discrimination. Science. 2005; 307:1121–1124. [PubMed: 15718474]
41. Smith WK. The functional significance of the rostral cingular cortex as revealed by its responses to electrical excitation. J Neurophysiol. 1945; 8:241–255.
42. Rudebeck PH, Buckley MJ, Walton ME, Rushworth MF. A role for the macaque anterior cingulate gyrus in social valuation. Science. 2006; 313:1310–1312. [PubMed: 16946075]
43. Vogt BA, Vogt L, Farber NB, Bush G. Architecture and neurocytology of monkey cingulate gyrus. J Comp Neurol. 2005; 485:218–239. [PubMed: 15791645]

44. Lee D, Rushworth MF, Walton ME, Watanabe M, Sakagami M. Functional specialization of the primate frontal cortex during decision making. J. Neurosci. 2007; 27:8170–8173. [PubMed: 17670961]

45. Fujiyama F, et al. Exclusive and common targets of neostriatofugal projections of rat striosome neurons: a single neuron-tracing study using a viral vector. Eur. J. Neurosci. 2011; 33:668–677. [PubMed: 21314848]

46. Graybiel AM. Habits, rituals, and the evaluative brain. Annu Rev Neurosci. 2008; 31:359–387. [PubMed: 18558860]

47. Rajakumar N, Elisevich K, Flumerfelt BA. Compartmental origin of the striato-entopeduncular projection in the rat. J. Comp. Neurol. 1993; 331:286–296. [PubMed: 8509503]

48. Matsumoto M, Hikosaka O. Lateral habenula as a source of negative reward signals in dopamine neurons. Nature. 2007; 447:1111–1115. [PubMed: 17522629]

49. Tye KM, et al. Amygdala circuitry mediating reversible and bidirectional control of anxiety. Nature. 2011; 471:358. [PubMed: 21389985]

50. Paton JJ, Belova MA, Morrison SE, Salzman CD. The primate amygdala represents the positive and negative value of visual stimuli during learning. Nature. 2006; 439:865–870. [PubMed: 16482160]

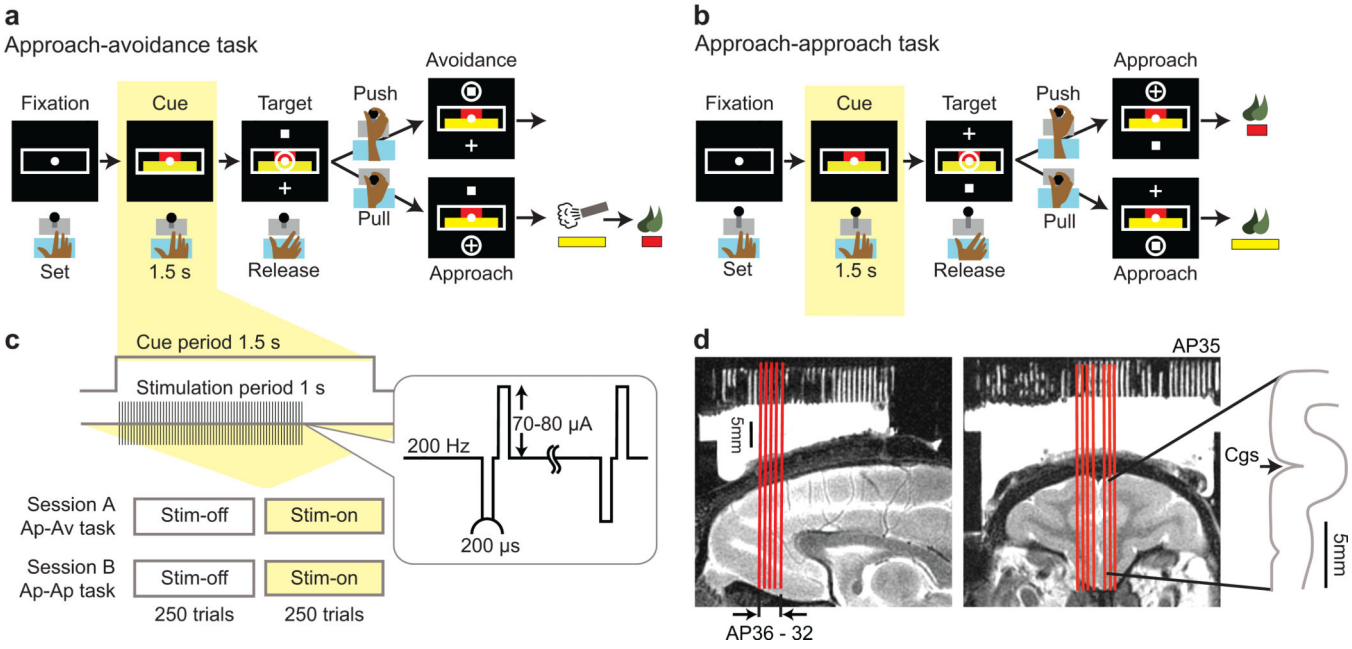

Figure 1.

Task procedures and recording regions. (**a**) Task flow diagram of the approach-avoidance (Ap-Av) task. The task started when the monkey put the hand on the home position. After 1.5-s fixation period, two bars appeared on the screen as a visual cue. The lengths of red and yellow bars indicated, respectively, the amount of liquified food and airpuff delivered after approach choice. After the 1.5-s cue period, the monkey could move the joystick to choose one target. Cross target indicated approach, and square target indicated avoidance. The locations of two targets were randomized across trials. After approach decisions, both airpuff and food were delivered in the indicated amounts. After avoidance decision, the monkey did not receive the indicated airpuff and food. (**b**) Task flow diagram of the approach-approach (Ap-Ap) task. The lengths of red and yellow bars corresponded to the amount of reward that the monkey could obtain after choosing cross and square targets, respectively. (**c**) Stimulation procedure. Daily sessions consisted of stimulation-off and stimulation-on blocks, each with 250 trials. In stimulation-on trials, microstimulation (a train of biphasic pluses; frequency: 200 Hz, current amplitude: 70–80μA) was applied for 1 s, starting at the onset of the visual cue. (**d**) Sagittal (left) and coronal (right) magnetic resonance images of the pregenual recording region. Red lines indicate estimated tracks of recording and stimulation electrodes ranging from AP 32 to AP 36. To the right, a schematic diagram of the pACC is shown with cingulate sulcus (Cgs).

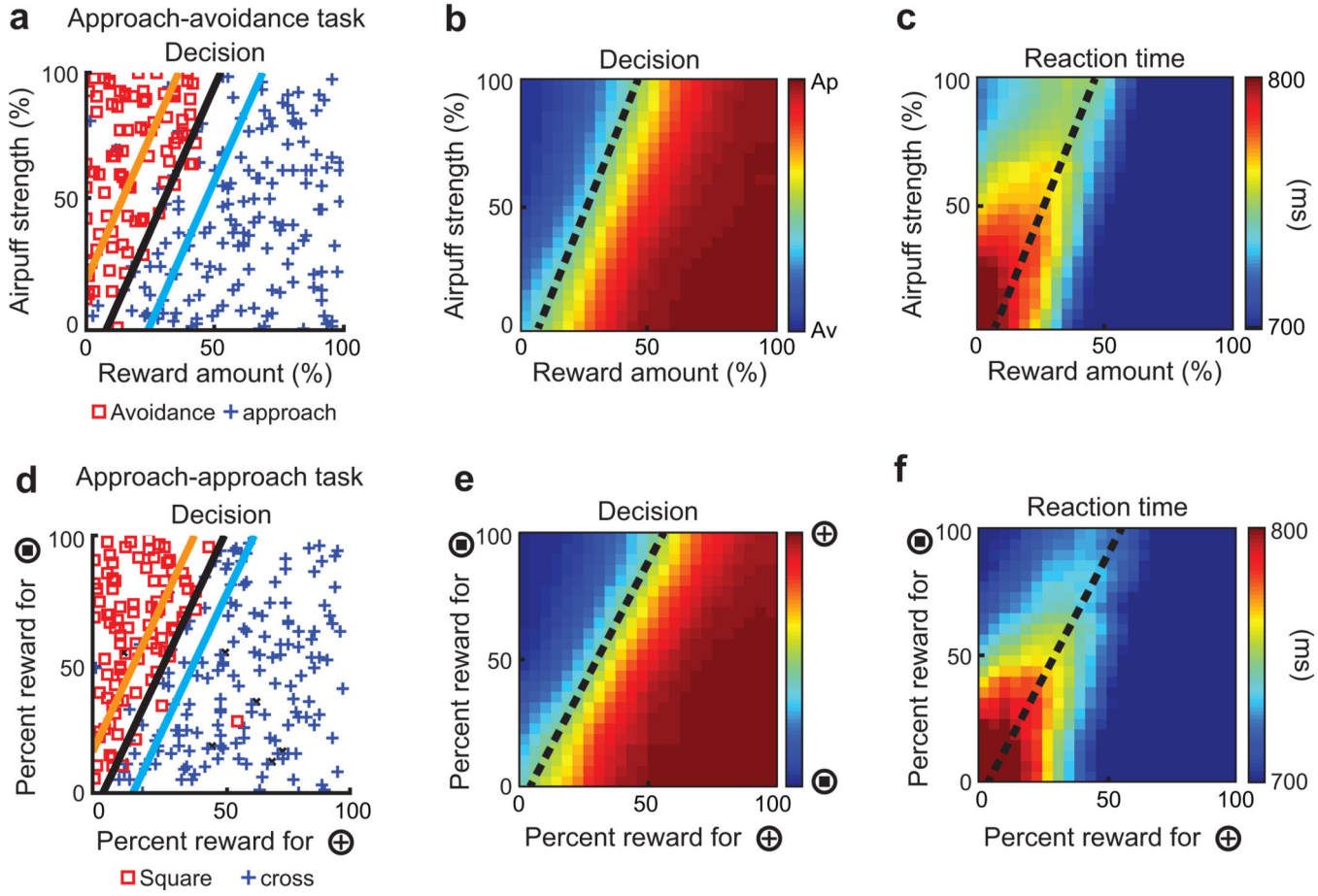

Figure 2.

Behavioral patterns. (**a**) Avoidance (red square) and approach (blue cross) choice made by monkey S in a single session of the Ap-Av task. Black line indicates the decision boundary calculated by logistic regression. Light blue and orange lines indicate 90% and 10% probability, respectively, of choosing approach estimated by the regression model. (**b**, **c**) Decision (**b**; red: approach, blue: avoidance) and reaction times (**c**; red: slow, blue: fast) averaged over all experiments for the Ap-Av task and plotted according to pseudocolor scales at right. Dotted lines indicate decision boundaries calculated based on all the accumulated data. (**d**) Choice of square (red square) and cross (blue cross) targets in a single session of the Ap-Ap task, by monkey S. Black, light blue and orange lines represent 50%, 90%, and 10% probabilities of choosing cross target, calculated by logistic regression. (**e**, **f**) Target choice (**e**) and reaction times (**f**) averaged over all Ap-Ap experiments. Dotted lines indicate decision boundary.

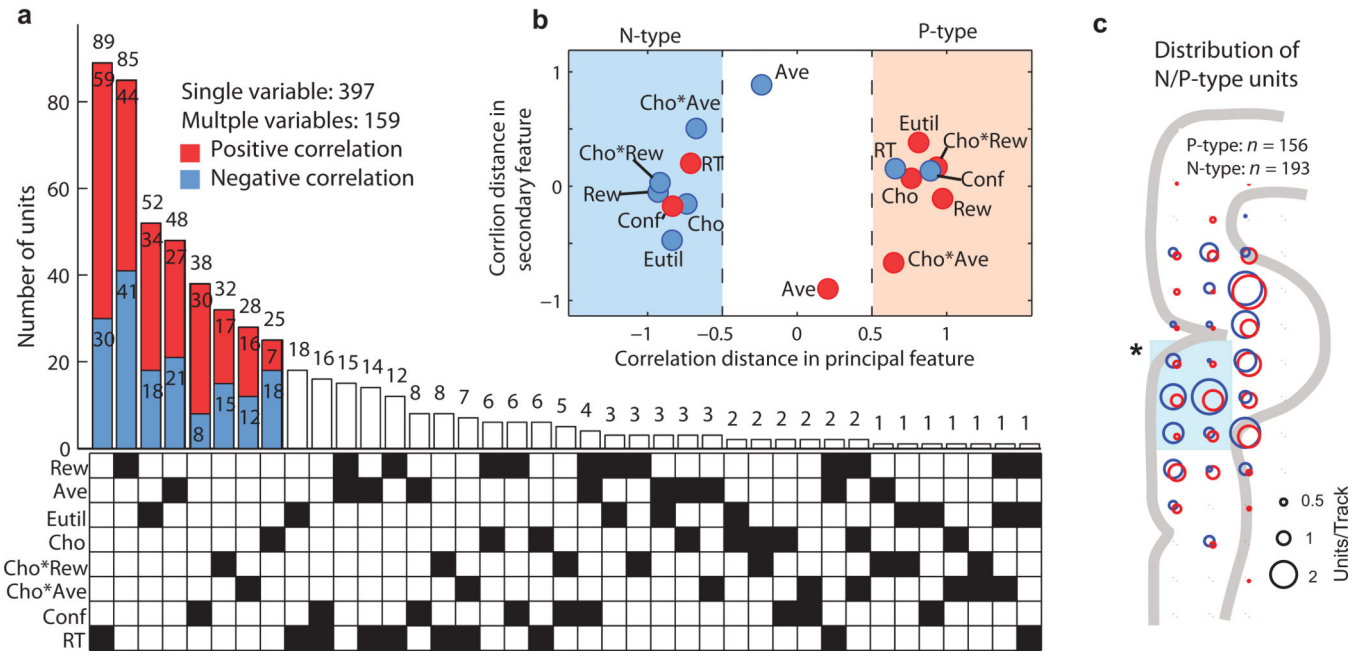

Figure 3.

Classification of units recorded in the pACC region. (**a**) Results of stepwise regression analysis for the Ap-Av task. Regression variables are offered reward (Rew), offered airpuff (Ave), choice (Cho), chosen reward (Cho*Rew), chosen airpuff (Cho*Ave), reaction times (RT), expected utility (Eutil) and conflict in decision (Conf). Y-axis indicates the number of recorded units best characterized by one or a combination of the variables identified in the matrix below. Black squares in the matrix along X-axis indicate the variable or variables selected by the stepwise regression procedure. Many units (397 units) were characterized by the single variables that we chose. These units were further classified by whether the activity was positively (red) or negatively (blue) correlated with the variable. Another 159 units were characterized by particular combinations of variables indicated by black squares in the matrix. (**b**) Results of multidimensional scaling performed based on the correlation distance of the firing patterns of each type of unit. X-axis shows the principal feature dimension, and y-axis shows the second feature dimension extracted by this procedure. Types of units located closely to each other indicate that their firing patterns are similar. Blue circles indicate the locations of units with activity negatively correlated with the indicated variable. Red circle indicate the locations of units with activity positively correlated with the indicated variable. Units were classified by the similarity derived in the primary feature, N-type (light blue region) and P-type (light red region). (**c**) Cortical distribution of N-type (blue circle) and P-type (red circle) units. In the ventral bank of the cingulate sulcus (blue shading), N-type units significantly outnumbered P-type units (Fisher's exact test, $P < 0.05$).

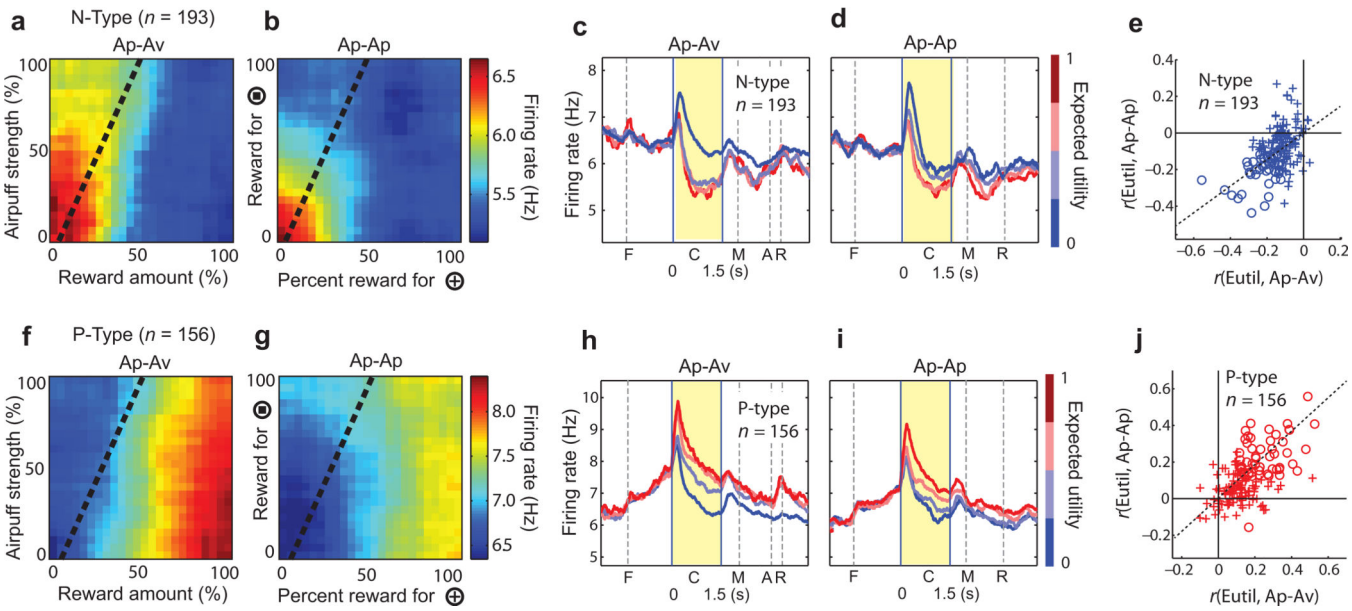

Figure 4.

Response properties of N-type (**a–e**) and P-type (**f–j**) units. (**a, b, f, g**) Population cue-period activity (color scale to right) of N-type (**a** and **b**) and P-type (**f** and **g**) units relative to the visual cue in the Ap-Av (**a** and **f**) and Ap-Ap (**b** and **g**) tasks. Black dotted line indicates the decision boundary. (**c, d, h, i**) Population activity across task-time for N-type (**c** and **d**) and P-type (**h** and **i**) units in the Ap-Av (**c** and **h**) and Ap-Ap (**d** and **i**) tasks. Line colors correspond to expected utility as indicated by color bar at right. Before averaging across sessions, the expected utility was normalized in each session so that the maximum expected utility is set to 1 and minimum expected utility to 0. F: fixation, C: cue, M: movement, A: airpuff, R: reward. Yellow shading indicates the cue period. (**e, j**) Scatterplots of correlation coefficients between cue-period activity and expected utility calculated for N-type (**e**) and P-type (**j**) units. Dotted line indicates regression slope. X-axis represents correlation coefficients between cue-period activity in the Ap-Av task and the expected utility calculated for the Ap-Av task. Y-axis represents correlation coefficients between cue-period activity in the Ap-Ap task and the expected utility calculated for the Ap-Ap task. Each circle indicates an N-type (**e**) or P-type (**j**) unit for which cue-period activity was significantly correlated with the expected utility calculated for both Ap-Av and Ap-Ap tasks (Pearson's correlation coefficients, $P < 0.05$). Cross indicates another unit that did not show a correlation between activity and utility in both tasks.

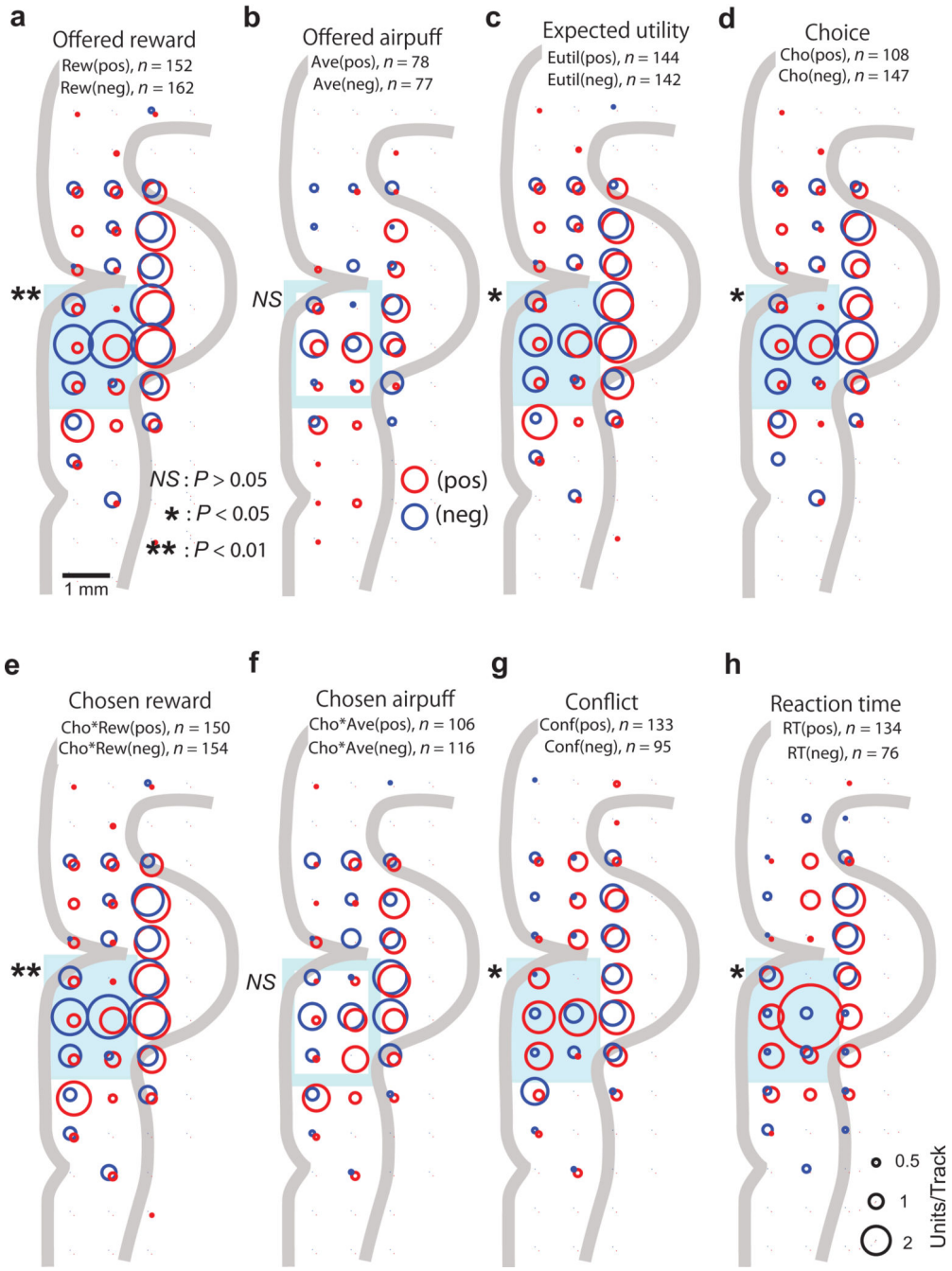

Figure 5.

Distributions of pACC units classified by the correlation analyses. Distributions and numbers (indicated by size of circles) of units whose activity showed significantly positive (red, pos-type) or negative (blue, neg-type) correlations (Pearson's correlation coefficients, $P < 0.05$) with offered amount of reward (Rew, **a**), offered strength of airpuff (Ave, **b**), expected utility (Eutil, **c**), approach or avoidance decision (Cho, **d**), amount of chosen reward (Cho*Rew, **e**), strength of chosen airpuff (Cho*Ave, **f**), conflict in decision (Conf, **g**), and reaction time (RT, **h**). Total numbers of correlated units are indicated (*n*). For each

distribution, we tested whether the neg-type or the pos-type populations of units in the ventral bank cortex significantly outnumbered the counterpart (blue shading, Fisher's exact test, $P < 0.05$) or not (blue rectangle).

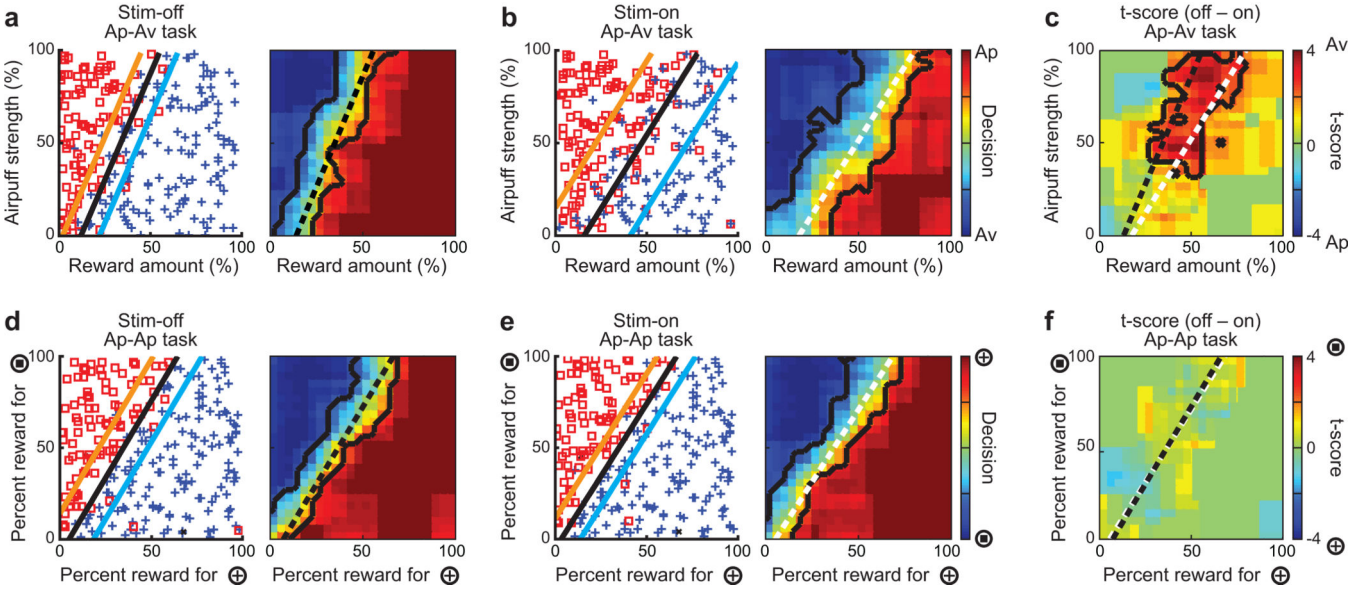

Figure 6.

Effects of pACC microstimulation on decision-making. Microstimulation (70 μA) was delivered during cue period at a single site (indicated by asterisk in Fig. 7a) in monkey S as she performed single Ap-Av (**a–c**) and Ap-Ap (**d–f**) task-sessions on consecutive days. (**a, b, d, e**) Left panels show scatter plots of each decision for stimulation-off (**a** and **d**) and stimulation-on (**b** and **e**) trials. Blue cross and red square indicate choice of cross and square targets, respectively. Black line indicates the session's decision boundary estimated by logistic regression analysis. Light blue and orange lines indicate the 90% and 10% levels, respectively, for choices of cross target, estimated by the modeled data produced by the logistic regression. Right panels show the mean choices for these stimulation-off (**a** and **d**) and stimulation-on (**b** and **e**) trials, with decision boundaries shown as dotted lines (black: stimulation-off, white: stimulation-on). Data were smoothed by a square window (20% by 20% of the decision matrix). Black outlines enclose decisions with 5% to 95% probability of cross target choices. (**c, f**) Matrix plots of t-scores demonstrating significant stimulation-induced increase in avoidance in the Ap-Av task (**c**), and lack of significant stimulation effect in the Ap-Ap task (**f**). Region outlined in black in **c** indicates zone with significant effects (Fisher's exact test, $P < 0.05$), which covered 16.6% of the entire data matrix.

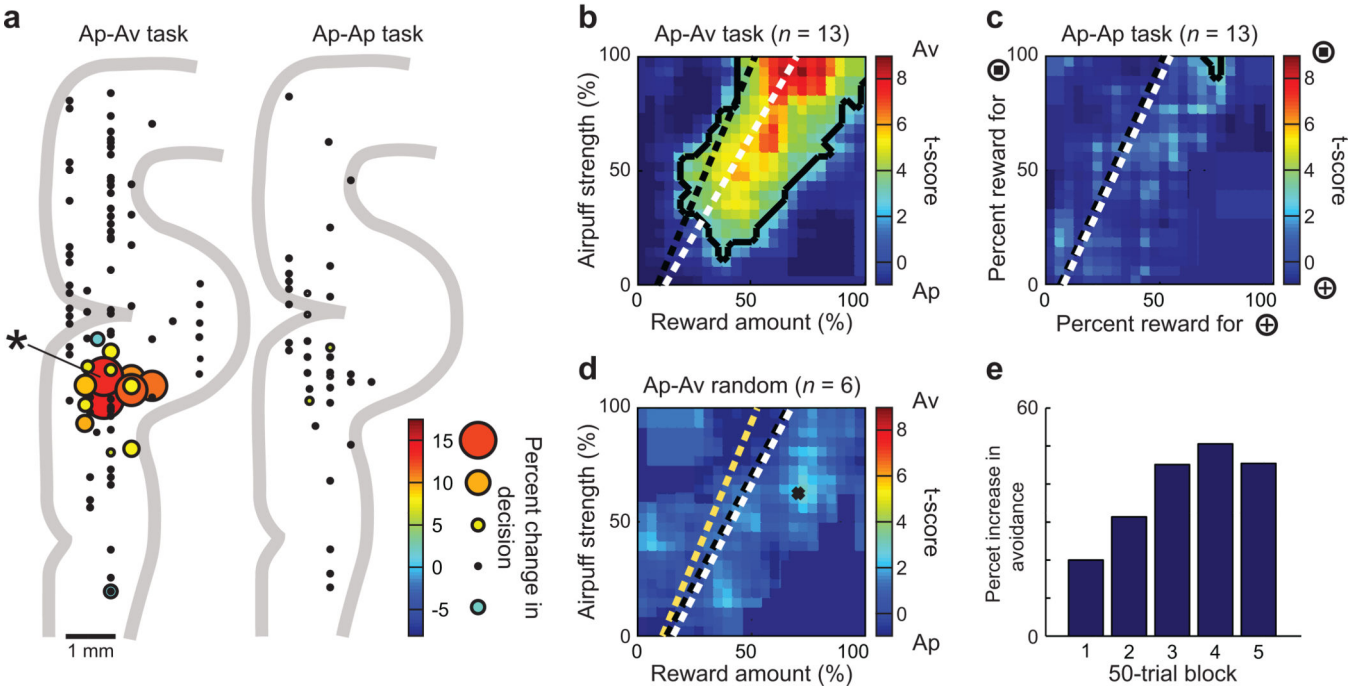

Figure 7.

Distribution and dynamics of stimulations affecting decision-making. (**a**) Distribution of all stimulation sites in Ap-Av (left) and Ap-Ap (right) tasks (current amplitude: 70–80 μA). Sizes and colors of circles indicate percentage of stimulation-induced change in decision (red-orange hues, increased avoidance; blue hues, increased approach). Circle centers show locations of monopolar electrodes or mid-points between bipolar electrodes. Black dots represent sites with less than 3% stimulation-induced change. Data collected from both hemispheres of monkeys S and A. (**b**) Average changes in decision shown for all ventral bank effective sites (n = 13), expressed as t-scores. Black outline surrounds significant data (Fisher's exact test, $P < 0.01$). Dotted lines indicate decision boundary (black: stimulation-off, white: stimulation-on). (**c**) Lack of stimulation-induced change in Ap-Ap task. (**d**) Lack of stimulation-induced difference in experiments with randomly presented stimulation-on trials (white dotted line) and stimulation-off trials (black dotted line). Yellow dotted line indicates decision boundary of collected data obtained in the stimulation-off trials in previous sessions. (**e**) Dynamics of stimulation effects on decisions for the 13 effective sites. Accumulated stimulation-on data were segregated into 5 temporal stages. Each bar represents the size of increase in avoidance in each of consecutive 50-trial stimulation-on blocks, relative to the 250-trial stimulation-off block.

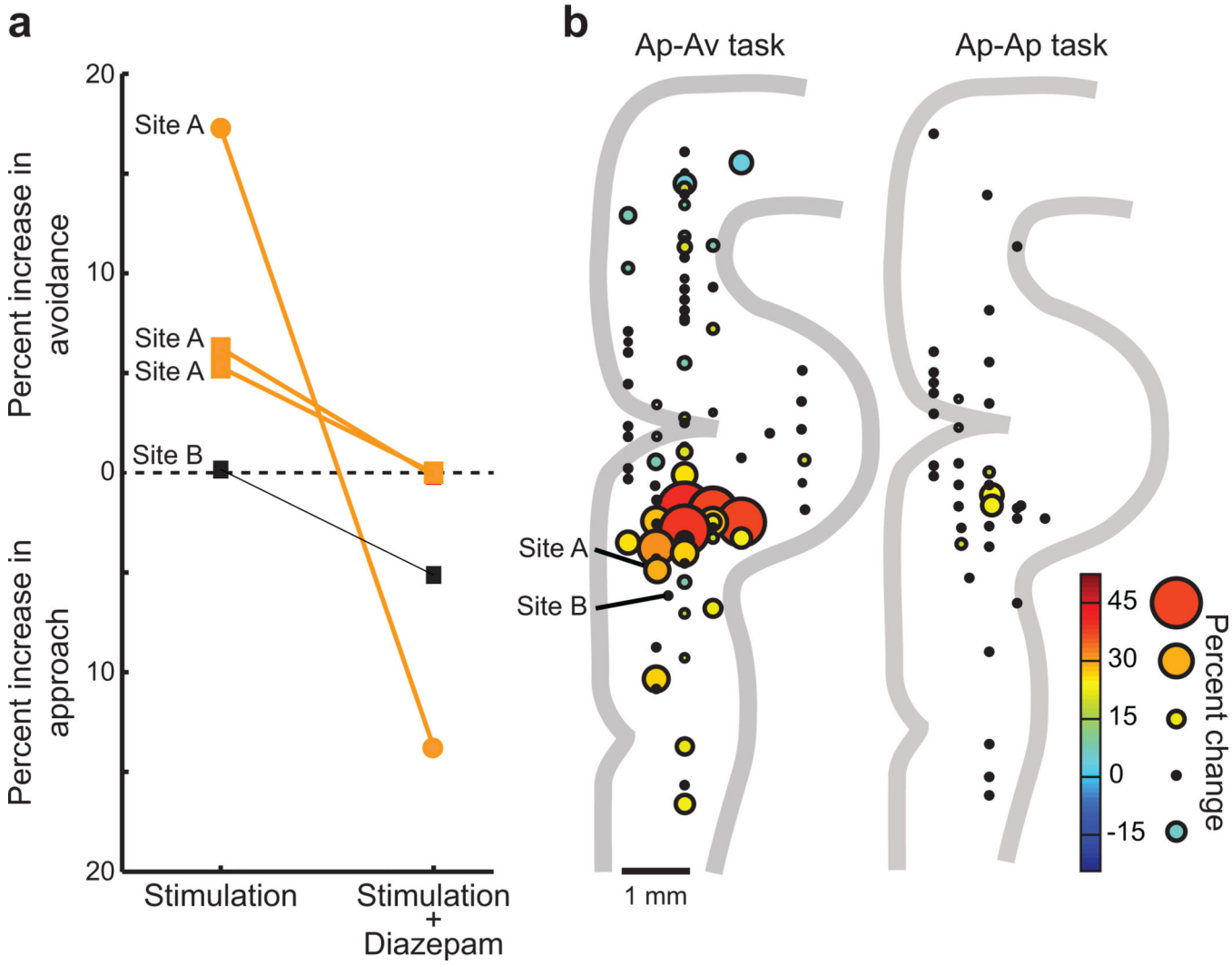

Figure 8.

Evidence suggesting potential negative affective state changes induced by microstimulation. (**a**) Effects of the anxiolytic, diazepam (0.25 mg/kg, IM), on the stimulation-induced change in the approach-avoidance decisions. Orange lines indicate the results of stimulation at site previously identified as an effective site A (square terminals: 80 μA, 2 sessions; circle terminals: 150 μA, 1 session) before and after diazepam treatment. Black line shows the result of diazepam treatment at ineffective site B, where stimulation (80 μA) did not induce a change in decision. Locations of sites A and B are shown in **b**. (**b**) Percent changes in the cost-benefit ratio defined by the ratio of sensitivities to offered airpuff and offered reward. The two sensitivities were derived from coefficients of the logistic behavioral model. Left panel: Ap-Av task (red-orange hues, increased sensitivity to aversive airpuff relative to reward; blue hues, increased sensitivity to reward relative to airpuff; black, no effect). Right panel: Ap-Ap task (yellow, increase in placing more value in square target; black, no effect).